Pure Appl. Geophys. 174 (2017), 679–700

DOI 10.1007/s00024-016-1433-6

Pure and Applied Geophysics

The Use of Geospatial Technologies in Flood Hazard Mapping and Assessment: Case Study from River Evros

Angeliki Mentzafou,[1] Vasiliki Markogianni,[1] and Elias Dimitriou[1]

Abstract—Many scientists link climate change to the increase of the extreme weather phenomena frequency, which combined with land use changes often lead to disasters with severe social and economic effects. Especially floods as a consequence of heavy rainfall can put vulnerable human and natural systems such as transboundary wetlands at risk. In order to meet the European Directive 2007/60/EC requirements for the development of flood risk management plans, the flood hazard map of Evros transboundary watershed was produced after a grid-based GIS modelling method that aggregates the main factors related to the development of floods: topography, land use, geology, slope, flow accumulation and rainfall intensity. The verification of this tool was achieved through the comparison between the produced hazard map and the inundation maps derived from the supervised classification of Landsat 5 and 7 satellite imageries of four flood events that took place at Evros delta proximity, a wetland of international importance. The comparison of the modelled output (high and very high flood hazard areas) with the extent of the inundated areas as mapped from the satellite data indicated the satisfactory performance of the model. Furthermore, the vulnerability of each land use against the flood events was examined. Geographically Weighted Regression has also been applied between the final flood hazard map and the major factors in order to ascertain their contribution to flood events. The results accredited the existence of a strong relationship between land uses and flood hazard indicating the flood susceptibility of the lowlands and agricultural land. A dynamic transboundary flood hazard management plan should be developed in order to meet the Flood Directive requirements for adequate and coordinated mitigation practices to reduce flood risk.

Key words: Flood hazard mapping, land use, GIS techniques, satellite imageries, transboundary river Evros, flood directive.

1. Introduction

During the last decades a debate has risen on the link between climate change and global warming and the increase of extreme weather events frequency (e.g. heat or cold waves, high winds, heavy rainfall). Although extreme weather events are integral part of the earth's climate system as a result of large scale atmosphere–ocean circulation patterns and their complex interaction with local weather and climate elements (Khandekar 2013), based on the latest IPCC (2013) "Summary for Policymakers" (SPM), the frequency or intensity of heavy precipitation events has *likely* increased in North America and Europe. Even though the conclusion of climate change contribution in worldwide extreme weather events is premature (Khandekar 2005), based on recent climate models the global warming will affect the hydrological cycle and increase the magnitude and frequency of intense precipitation events in most parts of Europe and especially in Mediterranean area (e.g. Semmler and Jacob 2004). This phenomena is expected to be intensified due to land use changes such as deforestation and urbanization, because although land use types are not directly involved in flood creation, they affect the water holding and infiltration capacities of the soil and therefore influence the flood intensity and propagation. As a result and also due to poor management practices concerning mainly dams operation, the flood risk and vulnerability tend to increase over many areas (Kundzewicz et al. 2010; Feyen et al. 2009). Wetlands are especially vulnerable to such pressures, due to their susceptibility to hydrological changes (Erwin 2009). The European Directive 2007/60/EC aims to the reduction and management of the risks that floods pose to human health, the environment, cultural heritage and economic activity and requires the assessment and management of flood risks. The flood risk management of transboundary water courses raises many challenges due to different approaches to strategic decision making, capacity and resources and

[1] Hellenic Centre for Marine Research, Institute of Marine Biological Resources and Inland Waters, 46.7 km Athens-Sounio Ave., 19013 Anavissos Attikis, Greece. E-mail: angment@hcmr.gr

due to the lack of a legal framework for cooperation and the public participation and awareness (UNECE 2009).

Natural hazards, such as floods, are multi-dimensional phenomena which have a spatial component (Meyer et al. 2009; Zerger 2002), and therefor GIS based multi-criteria decision analysis is an appropriate tool for processing spatial data on flood risk (Malczewski 2006; Papaioannou et al. 2015). Under this scope the flood hazard map of Evros transboundary river basin was produced after a grid-based GIS modelling method that aggregates the main factors related to the development of floods: topography, land use, geology, slope, flow accumulation and rainfall intensity (Kourgialas and Karatzas 2011). The verification of this tool was achieved through the comparison between the produced hazard map and the inundation maps derived from the supervised classification of Landsat 5 and 7 satellite imageries of four flood events that took place at Evros delta proximity, a wetland of international importance. Furthermore, the vulnerability of each land use against the flood events was examined. Geographically Weighted Regression has also been applied between the final flood hazard map and the major factors (geological structure, land uses, rainfall intensity, topography) in order to ascertain their contribution to flood events. Scope of this effort was to identify the flood prone areas of Evros transboundary watershed, to examine the effectiveness of the flood hazard mapping methodology proposed by Kourgialas and Karatzas (2011) at the specific case study and to assess the performance and the universality of this approach. Finally, the challenge of flood risk management in the transboundary catchment of Evros river is discussed.

2. *Study Area*

Evros river is the second largest river in Eastern Europe, flowing through Bulgaria, Greece and Turkey and discharging significant quantities of water and sediment in the Aegean Sea (Fig. 1). It emerges at the Rila mountain near the summit of Musala and flows first through a steep glacier valley and then east and southeast fringed by the Balkan and Rhodope mountains before crossing the Thracian plain (Skoulikidis et al. 2009). The total length of the river is about 528 km, 310 km of which belongs to Bulgaria and the remaining 218 km comprise the boundary between Greece and Turkey. The catchment area is about 53,000 km^2 while its annual average discharge fluctuates from 50 to 200 m^3/s. The most important tributaries of Evros river are Tundzha and Ardas in Erdine, Ergene in Ipsala and Erythropotamos near Didimoteicho (Dimitriou et al. 2010). Evros river basin is one of the most intensively cultivated areas in the Balkans and supports a population of 3.6 million people. Major pollution pressures comprise mining activities and untreated effluents from heavy and light industry at the Bulgarian part of the basin, industrial activities at the Turkish part, whilst in Greek part the cultivation activities make it one of the most import agricultural regions of Northern Greece (Dimitriou et al. 2011).

Evros delta, shared by Greece and Turkey, is one of the most important wetland on a national and European level. A major part of the delta in Greece is included in the list of wetlands designated as internationally important under the Ramsar Convention (1971), due to the numerous flora and fauna species hosted. Furthermore, Evros delta is designated as Special Protection Area (SPA) and as Site of Community Importance (SCI) in the Natura 2000 network (Dimitriou et al. 2010). Evros delta is also included in the list of wetlands of international importance of Turkey, while lake Gala in close proximity has been declared a National Park area (Ministry of Forest and Water Management of Turkey 2011).

Many dams and reservoirs are located along Evros river and its tributaries. In the Bulgarian part the total number of large dams and reservoirs is up to 722, mainly for hydropower production and secondarily for irrigation purposes and fish-breeding. In Turkey, seven dams and one regulator are under operation on the Ergene river and its tributaries, serving irrigation, flood control and some drinking water supply purposes, while also 53 small irrigation dams are located on several tributaries (UNECE 2011). In Greece the total number of small dams for irrigation purposes are five (Dimitriou et al. 2010).

The climatic and geomorphological conditions of Evros river basin lead to specific run-off conditions, characterized among others by high inter-annual flow variability (UNECE 2011). During the last decade

Figure 1
Evros river basin

and especially after 1994, the flood frequency and the dikes overtopping especially downstream of Evros river has increased dramatically (Angelidis et al. 2010), sometimes with severe social and economic impacts (Table 1). Among the most disastrous floods were in 2005 (returning period: 1000 years), in 2006 and in 2007 (UNECE 2011). It must be noted that it is not clear if this increase in the appearance of floods (six times greater frequency) is due to extreme climatic changes or a result of the management of the Bulgarian dams (Angelidis et al. 2010).

3. Methodology

3.1. Flood Hazard Mapping

The estimation of the flood-hazard areas of Evros river basin was accomplished after the methodology developed by Kourgialas and Karatzas (2011). The particular approach incorporates both dynamic and physical spatial properties to describe which areas of a catchment are more prone to floods than others. In this sense, lowland areas with impermeable lithology and high potential flow accumulation have higher flood risk than upstream areas, with higher slopes and permeable geological formations. Therefore, this GIS based multi-criteria decision analysis approach that is widely used, does not aim to present or predict a single flood event but to characterize the flood hazard of the entire catchment based on the protective functions provided by its physical and manmade characteristics.

Based on this approach, the flood-hazard map is produced after the integration of multi-criteria analysis at catchment scale with a grid-based GIS (Table 2). More specifically, six individual maps

Table 1

Major flood event of Evros river during the last decade

a/a	Begin date	End date	Areas affected	Main cause	Magnitude*	References
1	17/01/2003	03/03/2003	Northeastern Greece. Evros Prefecture. Tichero, Ampelakia, Chandra, Megali Doxipara, Mavrokklisi, Mandra, Thourio Southeastern Bulgaria Northwestern Turkey—Ergene River	Heavy rain	6.0	1, 2
2	17/02/2005	24/03/2005	Northeastern Greece—Thrace region. Evros Prefecture, Pytheio area, Sofiko district near Didymotichos. Lavra, Pitia and Poros Bulgaria—Maritsa river Northwestern Turkey—Odrin Tharace region.	Rain and snowmelt	5.6	1, 2, 3
3	02/01/2006	20/01/2006	Greece—Lavara, Kissario, Amorio, Tichero, Thymaria, Psathades in Didymotichos, Pythio, Trigono	Snowmelt	5.5	1, 2, 3
4	09/03/2006	25/03/2006	Northeastern Greece—Evros region. Thrace. Soufli Northwest Turkey—Edirne region. Tychero Southern Bulgaria—Kardzhali region, Haskovo, Plovdiv and Smolyan, Saedinenie	Rain and snowmelt	5.5	1, 2, 3
5	06/08/2007	–	Greece-Alexandroupoli—Makri	Heavy rain	–	3
6	16/11/2007	02/12/2007	Greece—Evros region, Eastern Macedonia and Thrace—Ghodopi, Rodopi, Komotini, Kavala and Drama. Turkey—Thracian and Aegean regions—Tekirdag. Edirne. Marmaris, Bodrum. Muğla province. Bulgaria—Stara Zagora—Radnevo, Galabovo, Tsarevo, Opan and Saedinenie. Sofia, Plovdiv, Burgas, Haskovo.	Heavy rain	6.0	1, 2
7	13/02/2010	20/02/2010	Greece—Evros rivers overflew. Traianoupoli, Ferres, Tichero, Soufli, Orfea, Didimoticho, Orestiada, Kiprinos, Vissa, Metaxades, Trigono Bulgaria—Tundzha River overflew its banks. Elhovo and its surrounding villages	Heavy rain	5.1	1, 2, 3
8	06/02/2012	11/02/2012	Greece—Dikaia, Ormenio, Ptelea, Orestiada—Trigono	Heavy rain	–	3
9	24/01/2013	04/02/2013	Greece—Alexandroupoli, Ferres, Doriskos, Loutro, Didimoticho, Sofiko	Heavy rain	–	3

* Flood magnitude = LOG (duration × severity × affected area)

1. Darmouth Flood Observatory (2014)

2. Ministry of Environment Energy and Climate Change (2012)

3. Ministry of Infrastructure, Transport and Networks—General Secretariat of Public Works—Earthquake Recovery Service (2014)

were produced for each of the main factors that contribute to the development of floods. These factors are: topography, land use, geology, slope, flow accumulation and rainfall intensity of the river basin. The effect of each factor is rated in five different hazard classes: very high, high, moderate, low and very low. In the case of numeric-valued factors (topography, slope, flow accumulation and rainfall intensity) the hazard classes were defined after Jenk's Natural Breaks method. This is dictated by the particular flood hazard methodology (Kourgialas and Karatzas 2011) but is also widely used in other similar modelling techniques for the estimation of flood and other natural disasters prone areas or during risk, hazard or vulnerability mapping (e.g. Mallick et al. 2015; Pasqualini et al. 2011; Stefanidis and

Table 2

Weight evaluation of the factors affecting flood-hazard areas proposed by Kourgialas and Karatzas (2011)

a/a	Factor	Domain of effect	Flood hazard	Weight of effect (w)	Rate (x)	Weighted rating ($w \times x$)	Total weight	Total weight (%)
1	Topography (m)	0–261.7	Very high	10	4.5	45	117	31.5
		261.7–557.4	High	8		36		
		557.4–944.2	Moderate	5		22.5		
		944.2–1,399.3	Low	2		9		
		1,399.3–2,901	Very low	1		4.5		
2	Land use	Zones seaward and artificial surfaces	Very high–high	10	3	30	78	21.0
		Shrub-brush-rangeland	High	8		24		
		Cropland and pasture	Moderate	5		15		
		Other agricultural land	Low	2		6		
		Mixed forest land	Very low	1		3		
3	Geology	Loose, silty porous formations	Very high-High	9	3	27	46.5	12.5
		Cohesive, sandy porous formations	Moderate	5		15		
		Fractured or karstic formations	Low-very low	1.5		4.5		
4	Slope (degrees)	0–3.0	Very high	10	2	20	52	14.0
		3.0–7.6	High	8		16		
		7.6–13.6	Moderate	5		10		
		13.6–21.2	Low	2		4		
		21.2–55.2	Very low	1		2		
5	Flow accumulation	1,198,798–2,333,539	Very high	10	1.5	15	39	10.5
		668,033–1,198,798	High	8		12		
		356,894–668,033	Moderate	5		7.5		
		100,662–356,894	Low	2		3		
		0–100,662	Very low	1		1.5		
6	Rainfall intensity (MFI)	75.3–98.9	Very high	10	1.5	15	39	10.5
		66.2–75.3	High	8		12		
		58.9–66.2	Moderate	5		7.5		
		52.8–58.9	Low	2		3		
		46.1–52.8	Very low	1		1.5		
Total							371.5	100.0

Stathis 2013). In cases of non-numeric valued factors (geology and land use) the hazard classes were defined according to the water infiltration capacity of the geological formations and land use types, after Kourgialas and Karatzas (2011) suggestions. The highly permeable geological formations and land use types were classified as of low and very low flood hazard while the low permeability formations and land use types were characterized as of high and very high flood hazard (Table 2). Afterward, for each factor a weight factor was attributed, depending again on their influence on flood processes. Finally, the flood-hazard map was produced after the aggregation of each weighted factor (Gemitzi et al. 2006) (Formula 1), while again the five flood hazard classes were defined after Jenk's Natural Breaks method.

$$S = \sum_{1}^{i} w_i x_i \quad (1)$$

where S: the hazard index, w_i: the weight of factor i, and x_i: the rate of factor i.

The flood hazard map concerning the elevation factor was developed in GIS environment using the digital elevation model (DEM) of the river basin of Evros (cell size 150 m). Likewise, the slope map was produced in GIS environment from the digital elevation model (DEM) of the study area. The drainage areas of a river basin can be indirectly determined by flow accumulation (Schäuble et al. 2008). The flow accumulation map was produced using the flow direction map, which was produced from the digital elevation model (DEM) of the river Evros river basin, in the ArcGIS 10.1 software.

The flood hazard map concerning land uses was developed based on CORINE 2000 database (European Environmental Agency 2012). The land uses proposed by European Environmental Agency were

Table 3

Assignment between Corine land use classes and land use classes used in Flood hazard mapping

Corine code	Corine description (level 3)	Land use classes (based on their sensitivity to flooding)	Flood hazard
111	Continuous urban fabric	Zones seaward and artificial surfaces	Very high
112	Discontinuous urban fabric	Zones seaward and artificial surfaces	Very high
121	Industrial or commercial units	Zones seaward and artificial surfaces	Very high
122	Road and rail networks and associated land	Zones seaward and artificial surfaces	Very high
124	Airports	Zones seaward and artificial surfaces	Very high
131	Mineral extraction sites	Zones seaward and artificial surfaces	Very high
132	Dump sites	Zones seaward and artificial surfaces	Very high
133	Construction sites	Zones seaward and artificial surfaces	Very high
141	Green urban areas	Shrub-brush-rangeland	High
142	Sport and leisure facilities	Shrub-brush-rangeland	High
211	Non-irrigated arable land	Cropland and pasture	Moderate
212	Permanently irrigated land	Cropland and pasture	Moderate
213	Rice fields	Cropland and pasture	Moderate
221	Vineyards	Other agricultural land	Low
222	Fruit trees and berry plantations	Other agricultural land	Low
231	Pastures	Cropland and pasture	Moderate
242	Complex cultivation patterns	Cropland and pasture	Moderate
243	Land principally occupied by agriculture, with significant areas of natural vegetation	Cropland and pasture	Moderate
311	Broad-leaved forest	Mixed forest land	Very low
312	Coniferous forest	Mixed forest land	Very low
313	Mixed forest	Mixed forest land	Very low
321	Natural grasslands	Shrub-brush-rangeland	High
322	Moors and heathland	Shrub-brush-rangeland	High
323	Sclerophyllous vegetation	Other agricultural land	Low
324	Transitional woodland-shrub	Other agricultural land	Low
331	Beaches. dunes. sands	Zones seaward and artificial surfaces	Very high
332	Bare rocks	Zones seaward and artificial surfaces	Very high
333	Sparsely vegetated areas	Other agricultural land	Low
411	Inland marshes	Zones seaward and artificial surfaces	Very high
421	Salt marshes	Zones seaward and artificial surfaces	Very high
511	Water courses	Zones seaward and artificial surfaces	Very high
512	Water bodies	Zones seaward and artificial surfaces	Very high
521	Coastal lagoons	Zones seaward and artificial surfaces	Very high
523	Sea and ocean	Zones seaward and artificial surfaces	Very high

categorized in the following five classes based on their sensitivity to flooding: seaward zones and artificial surfaces (very high), shrub-brush-rangeland (high), cropland and pasture (moderate), other agricultural land (low) and mixed forest land (very low), based on the assumption that limited vegetation cover indicates a very high flood hazard (Kourgialas and Karatzas 2011; Table 3; Fig. 2), since there is a nontrivial correlation between natural forest cover/-forest loss and flood frequency (Bradshaw et al. 2007).

The geological map of the study area was retrieved from the Geological Map of Greece, 1:500,000 (Institute of Geology and Mineral Exploration of Greece 1983), the Geological map of Turkey, 1:500,000 (General Directorate of Mineral Research and Exploration of Turkey 1961), and the Generalized Geology of Europe including Turkey (U.S. Geological Survey 2003). Likewise, the flood hazard map concerning the geological structure of Evros basin was developed based on the influence of each lithological formation at the flood processes, e.g. an area dominated by karstic formations is characterized by very low flood hazard potential (Kourgialas and Karatzas 2011). Different approaches for estimating rainfall intensity have been proposed, such as Fournier Index (Fournier 1960), Modified Fournier Index (Arnoldus 1980) and

Figure 2
Land uses of Evros river basin

Precipitation Concentration Index (PCI) (Oliver 1980). In this study, the rainfall intensity was estimated by using the Modified Fournier Index methodology (Arnoldus 1980), which together with Fournier Index, is the most commonly used index of rainfall aggressiveness (Morgan 2005; Formula 2). In order to determine the rainfall intensity, the meteorological data of 32 meteorological stations in Evros river basin were acquired (Table 4).

$$\mathrm{MFI} = \sum_{1}^{12} \frac{p^2}{p} \qquad (2)$$

where MFI: the modified Fournier index, p: the average monthly rainfall, and P: the average annual rainfall

The distribution of the rainfall stations covered quite satisfactorily the entire study catchment with the exception of the high altitudes since only 4 rainfall stations (12.5% of the total) were located above 800 m.a.s.l. In the present study, the spatial distribution of rainfall intensity was estimated based on spline interpolation method, which, comparing to other approaches (e.g. ordinary kriging, co-kriging and IDW—Inverse Distance Weighting), is considered to be the most appropriate for cases with a small number of data points (Kourgialas and Karatzas 2011). The location and altitude of the available stations represented quite well the topography and geographical coverage of the particular catchment (Tables 4, 5; Fig. 3) which therefore is reflected to the interpolated maps. The density of raingauges network is about 1660 km^2/station and can be considered as sufficient, based on WHO (2008) recommended minimum densities of recording precipitation stations. Another limitation is the lack of snowmelt measurements which is a significant source

Table 4

Meteorological stations at Evros river basin

a/a	Meteorological Station	*X* (EGSA)	*Y* (EGSA)	X (°)	*Y* (°)	*z* (m)	Country	MFI
1	Borovets	468,502.94	4,677,319.18	23.62	42.25	1346	BG	80.97
2	Botev	575,178.64	4,729,848.01	24.92	42.72	2376	BG	98.99
3	Cerkezkoy	834,815.86	4,578,386.89	28	41.29	170	TR	55.29
4	Chirpan	609,654.18	4,672,553.68	25.33	42.20	173	BG	52.52
5	Corlu	818,667.05	4,563,863.50	27.80	41.17	183	TR	54.44
6	Didimoteicho	708,998.27	4,580,341.39	26.50	41.35	25	GR	48.90
7	Edirne	712,998.46	4,614,908.40	26.56	41.66	48	TR	53.10
8	Elhovo	712,099.72	4,672,674.19	26.57	42.18	138	BG	47.31
9	Ferres	682,297.01	4,529,628.68	26.17	40.90	26	GR	58.31
10	Haskovo	629,978.66	4,645,131.69	25.57	41.95	230	BG	57.12
11	Hayrabolu	760,328.30	4,566,816.91	27.11	41.21	–	TR	58.34
12	Ihtiman	485,043.92	4,697,251.53	23.82	42.43	636	BG	52.39
13	Kardjali	611,381.40	4,609,534.60	25.34	41.63	–	BG	62.02
14	Karnobat	744,130.74	4,725,970.54	26.98	42.65	198	BG	49.84
15	Kazanluk	614,664.77	4,719,283.32	25.40	42.62	380	BG	53.79
16	Kiprinos	685,741.71	4,605,595.02	26.23	41.58	70	GR	55.44
17	Kırklareli	768,497.76	4,624,556.84	27.23	41.73	232	TR	51.60
18	Koprivshtitsa	529,364.44	4,720,617.09	24.36	42.64	945	BG	68.40
19	Lefkimi	684,797.62	4,544,132.92	26.20	41.03	150	GR	76.52
20	Luleburgaz	779,902.83	4,588,294.16	27.35	41.40	46	TR	56.42
21	Orestiada	711,021.38	4,597,069.06	26.53	41.50	43.5	GR	48.50
22	Panagyurishte	513,807.67	4,710,574.56	24.17	42.55	562	BG	57.83
23	Pazardjik	526,364.29	4,668,406.07	24.32	42.17	205	BG	48.23
24	Peshtera	525,179.76	4,653,197.65	24.31	42.03	436	BG	53.79
25	Plovdiv	561,818.26	4,666,418.09	24.75	42.15	160	BG	46.20
26	Sadovo	578,343.15	4,666,582.61	24.95	42.15	158	BG	48.31
27	Sliven	689,718.75	4,726,488.20	26.32	42.67	226	BG	51.90
28	Smolyan	556,532.94	4,603,450.07	24.68	41.58	1180	BG	79.45
29	Soufli	692,706.47	4,563,223.97	26.30	41.20	15	GR	69.01
30	Stara Zagora	633,954.63	4,697,412.34	25.63	42.42	166	BG	52.43
31	Svilengrad	682,710.43	4,626,294.00	26.20	41.77	54	BG	53.00
32	Yambol	706,982.82	4,705,864.86	26.52	42.48	143	BG	46.95

Table 5

Main statistical values of the study area Rainfall stations

	Bulgaria	Greece	Turkey	Annual Rainfall (mm)		MFI
No of stations	20	6	6	Min	515	46
Mean altitude (m)	512	55	136	Max	1085	99
Min altitude (m)	54	15	46	Range	570	53
Max altitude (m)	2376	150	132	Mean	656	60
Mean Rainfall (mm)	672	665	600	Median	598	55
Max Rainfall (mm)	1085	942	713	StDev	136	13
				25th perc.	564	52
				75th perc.	710	68

of water for the hydrographic network during spring and early summer. In most cases, for the flood hazard estimation, snowmelt is not the crucial factor since the methodology focuses on flash floods which are mostly caused by short in duration, high rainfall intensity events. Therefore, the importance of rainfall and rainfall intensity is apparent in the methodology since it comprises one of the 6 dominant factors for assessing flood risk and affects the output risk map by approximately 11% (total weight of this parameter,

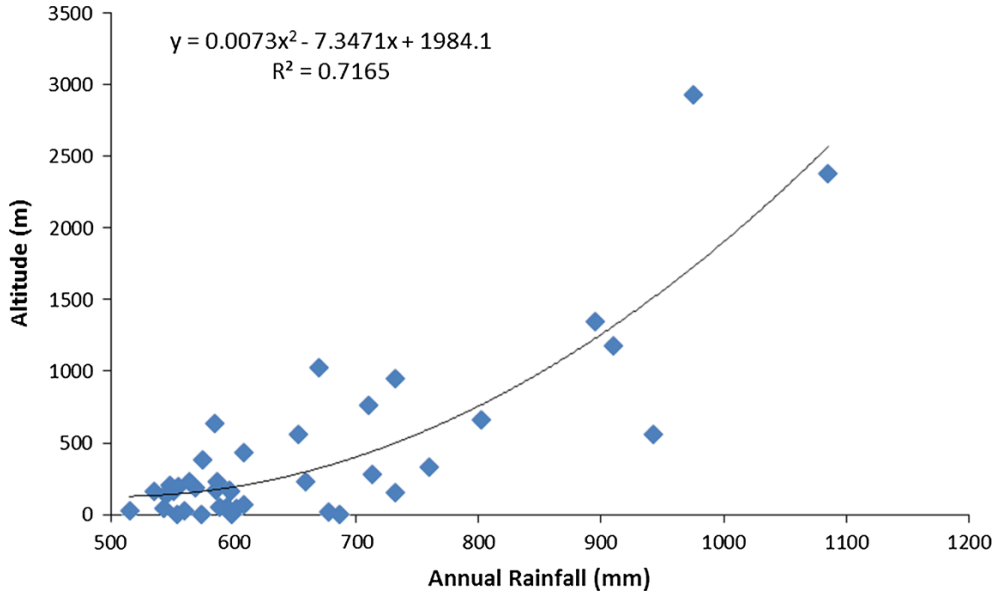

Figure 3
Relationship between Mean Annual Rainfall and Altitude in the study area

Table 2). However, there are many other factors that are taken into account such as slope, land use and topography that also affect the flood risk estimation and amend the effect of high rainfall intensity in areas of relatively low risk (e.g. steep hillslopes, top of mountains, etc.).

3.2. *Validation of Flood Hazard Mapping Methodology—Satellite Images*

The verification of the specific flood hazard mapping methodology was achieved through the comparison between the produced hazard map and the inundation maps derived from the supervised classification of Landsat 5 and 7 satellite imageries of four flood events. The area examined was the riparian zone of the downstream part of the catchment, a 10,000 m buffer zone along the main Evros river thalweg, from Evros delta to the triple point border between Greece, Turkey and Bulgaria. The floods events examined were selected based on their magnitude (Table 1), but also based of the availability of satellite images to cover the specific flood events sufficiently. The flooded event chosen were: a) 17/01-03/03/2003 (date of satellite image retrieved: 03/03/2003), b) 17/02-24/03/2005 (date of satellite image retrieved: 25/03/2005), c) 09-25/03/2006 (date of satellite image retrieved: 13/04/2006), and d) 13-20/02/2010 (date of satellite image retrieved: 19/02/2010).

Six Landsat 5 imageries (two for each date) of 25/03/2005, 13/04/2006 and 19/02/2010 and two Landsat 7-SLC-on of 03/03/2003 with cellsize of 30 m were acquired from the United States Geological Survey (USGS) under a clear sky and windy conditions. The data elaboration and analysis was conducted in ESRI's ArcGIS 10.1 software while for the analysis of the satellite imagery ENVI 4.7 software was used. After selecting the study area scenes and the appropriate dates the digital data were submitted to the following procedures:

1. Georeferencing of the imagery and geographical conversion from WGS'84 to EGSA'87 coordinate system (National Datum) were performed using Beam 4.7 software.
2. Radiometric correction for the conversion of actual radiance values, based on the formula [3] (YCEO 2010).

$$L_\lambda = \{(L_{\mathrm{Max}\lambda} - L_{\mathrm{Min}\lambda}) / (Q_{\mathrm{CALMAX}} - Q_{\mathrm{CALMIN}})\} \times (Q_{\mathrm{CAL}} - Q_{\mathrm{CALMIN}}) + L_{\mathrm{Min}\lambda} \quad (3)$$

where L_λ is the cell value as radiance, Q_{CAL} is the digital number, $L_{MIN\lambda}$ is spectral radiance scales to Q_{CALMIN}, $L_{MAX\lambda}$ is spectral radiance scales to Q_{CALMAX},Q_{CALMIN} is the minimum quantized calibrated pixel value (typically = 1), Q_{CALMAX} is the maximum quantized calibrated pixel value (typically = 255)

3. Atmospheric correction, through the darkest-pixel subtraction technique (Keiner and Yan 1998; Lathrop et al. 1991) via the relevant ENVI 4.7 software tool.
4. Satellite bands of each imagery with the same resolution (m) were joined in a single layer (layer stacking) and stored in image format (Tiff, Geotiff).

Supervised and unsupervised classifications were used to detect the flooded areas. As far as the unsupervised classification is concerned, K-MEANS classification algorithm was used to classify the water-covered from the dry riparian areas for the imageries on 25/03/2005, 13/04/2006 and 19/02/2010. Respectively, supervised classification and particularly Spectral Angle Mapper (SAM) (Becker et al. 2007; Castillejo-González et al. 2009; Debba et al. 2005) was used to detect the aforementioned differentiation of 03/03/2003. K-MEANS classification algorithm has been selected after several test runs and comparison with the results provided by other commonly used algorithms such as Iterative Self-Organizing Data Analysis (ISODATA). With regards to the supervised classification, groups of pixels (ROIs) or individual spectra should be selected as representative areas or materials to be mapped in the output. In this paper the selection of ROIs was selected with great attention even for the different shades of water. Also, SAM has been selected after comparison with the results of other supervised classification techniques, including parallelepiped, minimum distance and maximum likelihood. The classification result was four maps with the inundated areas that were superimposed for comparison purposes to the flood hazard map.

Flooded areas classification was carried out in the riparian zone with medium analysis (spatial resolution 30 m) in order for the wet in the riparian zone to be accurately quantified. Moreover, in order to quantify each classification errors, random points were created inside the inundated areas of each imagery. Creating random points is widely used concerning the classification accuracy assessment (Gass et al. 2013; Turner et al. 2013). The randomness of the selection is achieved by the ArcGIS relevant algorithm (Michigan Technological University 2011) where the user declares the number of points, the minimum distance between them as well as the reference zone (constraining feature class) within which the points will be contained (inundation areas in this case). Taking into consideration the spatial resolution of the satellite imageries (30 m) and the extent of the buffer zone along the main Evros river, it was estimated that 400 points needed to be created in order to have a 30-m minimum distance among them and cover spatially the whole area. This procedure resulted in a satisfactory density of check points (5 points/km^2) and subsequently followed the estimation of the percentage agreement with the actual flooded areas.

3.3. *Geographically Weighted Regression*

There are a number of assumptions underlying the basic regression model, one of which is that the observations should be independent of one another. This is not always the case with data for spatial units and not only might the variables in the model exhibit spatial dependence (that is, nearby locations will have similar values) but also the model's residuals might exhibit spatial dependence. The latter characteristic can be observed if the residuals from the basic regression are plotted on a map where commonly the residuals in neighboring spatial units will have a similar magnitude and sign (Charlton and Fotheringham 2009). The difference between Geographically Weighted (GWR) and multiple linear regression is that GWR incorporates the spatial aspect of the elaborated parameters and thus the produced regression is weighted according to their geographical location. Geographically weighted regression (GWR) is a recent refinement of ordinary regression model, describes relationships among variables that are different concerning their location (Fotheringham et al. 2002) and is used to model spatially varying relationships.

Geographically Weighted Regression (GWR) is a fairly recent contribution to modelling spatially heterogeneous processes (Brunsdon et al. 1996; Fotheringham et al. 1996, 1997, 2002). The underlying idea of GWR is that parameters may be estimated anywhere in the study area given a dependent variable and a set of one or more independent variables which have been measured at places whose location is known. Parameters that were analyzed and correlated in the GWR model with the flood hazard map were the topography, land uses, geology, flow accumulation and rainfall intensity (MFI index) of the Evros river basin. Concerning the geology and the land use parameters, reference numbers have been attributed to each geological and land use type, respectively. Thus, the reference number of each land use or geological formation was correlated with the respective flood hazard index. As far as the input parameters are concerned, the Kernal type (Gaussian) that was selected is the fixed one and it has been determined using the Akaike Information Criterion (AICc; Bandwidth method). AIC serves as an approximately unbiased estimator in instances where the sample size is large and the dimension of the candidate model is relatively small (Davies et al. 2005a). Davies (2002) and Davies et al. (2005b) show that AICc is the minimum variance unbiased estimator of its target discrepancy in a linear regression framework. All the aforementioned parameters were correlated via the relevant ArcGis 10.1 tool, the local coefficient of determination (R^2) was mapped for each one at a catchment scale and the global R^2 was also computed. Statistical report with diagnostic parameters was also generated and a comparative assessment followed to identify the dominant factors that are mostly correlated with the flood hazard map of Evros river basin.

4. Results

4.1. Meteorological Data

The mean annual rainfall of the study area reaches 656 mm while the maximum annual rain (1,085 mm) is observed in a Bulgarian station at an altitude of 2,376 m (Table 5). The minimum rainfall value (515 mm) is observed in a Greek station located at an altitude of 25 m while the correlation between the annual mean rainfall and the stations altitude is well described with a 2nd order polynomial with a R^2 of 0.72 (Fig. 3). The effect of the annual and monthly rainfall values on the MFI index is direct due to the algebraic dependence between these parameters and therefore MFI values illustrate almost identical distribution with the rainfall. Thus, 50% of the stations illustrate a MFI index of up to 55 with a maximum of 99, while 25% of the stations reach a value of 52 (Table 5). The distribution of MFI illustrates a positive skewness and more than 40% of the stations illustrate elevated MFI values that fluctuate above 60. Practically, this means that the study area presents favorable conditions for flood occurrences since it illustrates relatively high rainfall intensities which are counterbalanced though from the relatively low rainfall heights.

4.2. Flood Hazard Mapping

Based on the methodology mentioned above, the following six maps (one for each factor, Fig. 4a–f), which are directly related to flood events, and the final flood hazard map were developed (Fig. 4g).

Although low and very low are the dominant flood hazard classes of Evros river basin, the areas characterized by high and very high flood hazard are significant (19.1 and 6.1%, respectively). Based on the flood hazard map produced, the areas with very high flood hazard potential are (Fig. 4g): (1) the wider Evros delta region, (2) the area located within a zone of few kilometers along the riparian zone of Evros river from delta until Soufli village in Greece, (3) locally along Ardas river in Greece and Bulgaria, (4) the wider area around Edirne city, after the junction of Evros river (Maritsa) from Bulgaria, Ardas river from Greece and Tundzha from Turkey, (5) the wider riparian zone along Ergene river in Turkey, (6) the area around the city Keşan, east of Evros delta at Turkey, where rice field and wetlands are located, (7) along Hayrabolu stream in Turkey, (8) the regions around the cities Plovdiv, Saedinenie and Pazardjik in Bulgaria, and (9) at the coal mines Maritsa Iztok in Bulgaria. Thus, the dominant land uses in the very high flood hazard areas are urban

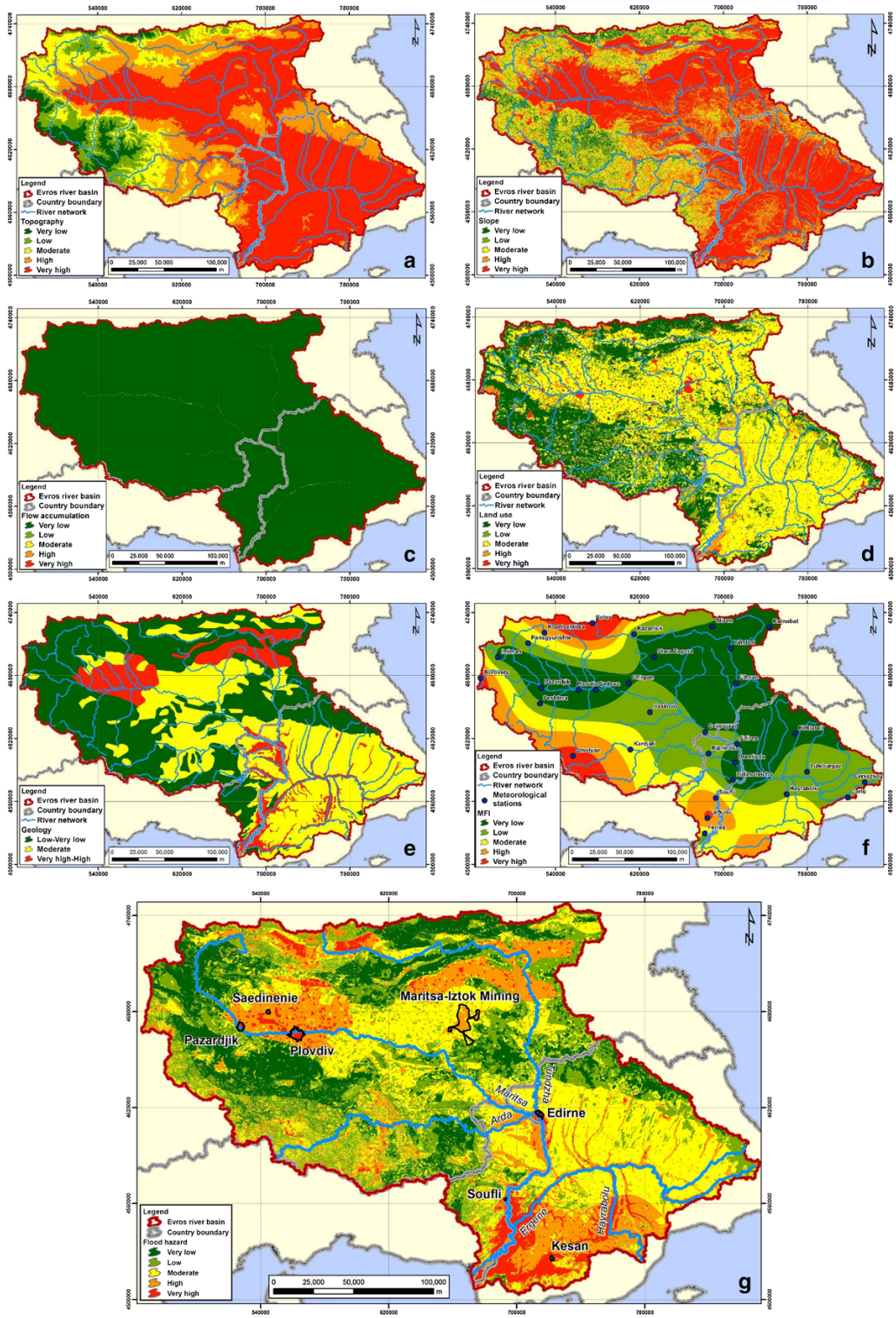

Figure 4
Flood hazard maps of each factor (**a**: topography, **b**: slope, **c**: flow accumulation, **d**: land use, **e**: geology, **f**: rain intensity MFI) and final flood-hazard map for Evros river basin (**g**)

areas followed by agricultural areas and wetlands (Table 8).

4.3. Validation of Flooded Areas Classification

Flooded areas classification was carried out in the riparian zone with medium analysis (spatial resolution 30 m) in order water -covered areas in the riparian zone to be accurately quantified. The elaboration result was quite good and the derived flood maps of each date showed that there were relatively few errors after they were compared carefully with the background of the satellite images. Moreover, in order to quantify the exact estimation errors of each classification, 400 random points were created for each flood map. As far as the flood of 03/03/2003 is concerned, only 19 points from the 400 were located outside flooded areas. Similarly, floods of 13/04/2006, 19/02/2010 and 25/03/2005 presented only 10, 6 and 8 points, respectively that were located away from flooded areas. The percentage estimation errors are 4.75, 2.5, 1.5 and 2% for the classification of flooded areas of March 2003, April 2006, February 2010 and March 2005.

It must be noted that even though the period between the flood's and the satellite image acquisition's date is in some cases fairly long, the remaining remote sensed flooded areas coincide with the flood endangered areas, thus the good performance of the model is verified.

4.4. Geographically Weighted Regression (GWR) Between Flood Hazard Map and Environmental Parameters

The GWR between overall flood hazard map and the numerically transformed, geological map of Evros river basin is positive with local R^2 ranging from 0 to 0.14. Values of R^2 are low, indicating the absence of a strong relationship between the aforementioned parameters (Table 6, Fig. 5a). The highest values though (0.14) are presented at the same areas where porous formations (quaternary, neogene and paleogene sediments) are dominant (western part of Evros river basin) while the lowest ones coincide with Triassic, Paleozoic and metamorphic formations and cretaceous sediments (at northern and central part). Concerning the global regression that GWR tool

Table 6

GWR indices between flood hazard map and environmental parameters

Variable	Geology	Land uses	Rainfall intensity—MFI	Topography	Flow accumulation
Bandwidth	28,701.55	24,969.11	23,115.7	24,131.6	43,358.58
Residual Squares	1,380,538.54	149,422.21	118,783.9	5,454,713,883.3	67,806.18
Effective Number	53.51	73.1	82.1	240.97	11.86
Sigma	16.75	9.31	5.2	240.64	17.24
AICc	42,199.9	13,145.031	27,676.2	1,303,897.98	2055.7
R^2	0.23	0.26	0.79	0.85	0.47
R^2Adjusted	0.22	0.23	0.79	0.85	0.45

Explanation of GWR diagnostics

Bandwidth: is the bandwidth of neighbors used for each local estimation and controls the degree of smoothing in the model

Residual Squares: this is the sum of the squared residuals in the model and the smaller this measure, the closer the fit of the GWR model to the observed data

Effective number: this value reflects a tradoff between the variance of the fitted values and the bias in the coefficient estimates and is related to the choice of bandwidth

Sigma: this value is the square root of the normalized residual sum of squares where the residual sum of squares is divided by the effective degrees of freedom of the residual

AICc: this is a measure of model performance and is helpful for comparing different regression models

R^2: R-squared is a measure of goodness of fit. It may be interpreted as the proportion of dependent variable variance accounted for by the regression model

R^2 Adjusted: calculations for the adjusted R-squared value normalize the numerator and denominator by their degrees of freedom

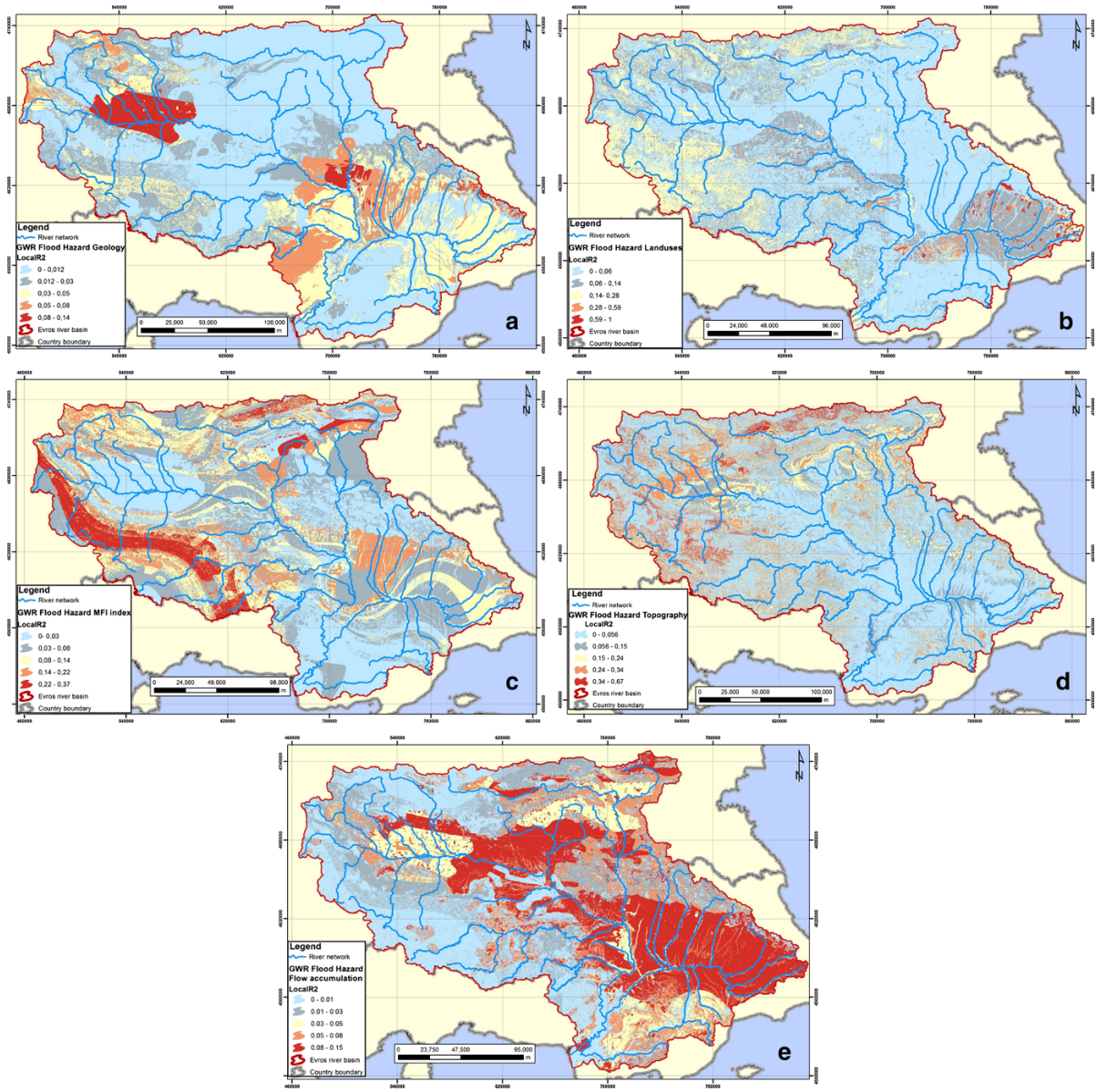

Figure 5
Cartographical representation of determination coefficient (R^2) between flood hazard map of Evros river basin and **a** geological formations, **b** land uses, **c** MFI index, **d** topography and **e** flow accumulation

simultaneously executes, global R^2 is equal to 0.23, value slightly greater than the local one. By means of GWR, having transformed the data in this way it is now possible to investigate local trends in non-stationarity in regression models, something that would not have been obvious from the raw data. Thus, like the Fourier Transform, it is a data transform that may be used to look at a data set from a different viewpoint (Brundson et al. 1996). The technique can also be seen as a response to calls such as Fotheringham (1992), Fotheringham and Rogerson (1993), and Openshaw (1993) for a move away from whole-map statistics to localized statistics which are more informative and which can be mapped.

Regarding GWR between the overall flood hazard map and the numerically transformed land use map of Evros river basin, local R^2 range from 0 to 1, presenting obviously a stronger relationship than the geology parameter (Table 6; Fig. 5b). Areas with the highest correlation (0.59–1) are mainly located where industrial, commercial units and sparsely vegetated areas are detected (eastern part of catchment). Moderate correlation was observed at those areas where permanently irrigated land exists (western part). The global coefficient differs from the local and equals to 0.26, indicating a low-moderate relationship. This difference in local–global R^2 (also regarding the GWR of flow accumulation), exists because GWR expands traditional regression by allowing the assessment of local and not global parameters (Fotheringham and Brunsdon 1999). This regression type controls the existence of spatial nonstationarity in the relationship between independent and dependent variable, enabling spatial change of independent variables' parameters (De Smith et al. 2007).

GWR between the flood hazard map and the rainfall intensity index generated R^2 values ranging from 0 to 0.37, indicating a moderate spatial relationship (Table 6; Fig. 5c). The highest R^2 values (0.22–0.37) are detected at those areas with a moderate rainfall intensity, mainly in the northern and southwestern part of the catchment. The lowest values of coefficient of determination, coincide with the areas that are characterized by the smallest rainfall intensity in the northeastern part of Evros river basin. On the contrary, global regression for the above parameters is higher than the local and equals to 0.79, value revealing a strong interrelationship between the above parameters. GWR focuses on exploring local differentiations and not on the ascertainment of any spatial uniformity. Accepting the fact that each location is characterized by different spatial features, the transition analysis from the global to local scale is enhanced by introducing the spatial parameter (location), hence local regression takes into consideration the location in contrast to the global. Thereby can this difference between local and global R^2 be explained and moreover in this case it indicates that the flooded areas are mostly affected by the cumulative rain of their upstream part of catchment rather than the local rainfall intensity patterns.

The coefficient of determination yielded from the GWR between the flood hazard map and topography ranges from 0 to 0.67, and the areas with the highest values coincident with those of the greatest elevation (2000–2900 m), in the western part of Evros river basin (Table 6; Fig. 5d). The parameter of topography is very important in the assessment process, accompanied by the highest weight, for the generation of the flood hazard map, accredited also by the aforementioned high value of the coefficient of determination. Similar interrelationship is also revealed through the global R^2 which equals to 0.85 and confirms the flood hazard dependence on the topography of the area.

Similar R^2 values (0–0.15) were resulted from the GWR analysis between the flow accumulation and the flood hazard map, indicating a weak relationship in contrast with the global R^2 value (0.47), which reveals a moderate one. The highest values of the correlation coefficient (0.15) appear, as it was expected, at those areas characterized by the greatest flow accumulation values and denser hydrographic network (Fig. 5f).

4.5. *Validation of Flood Hazard Mapping Methodology*

Based on the inundated areas produced from the satellite images, the flood events with the greatest extent was observed on 19/02/2010 and on 13/04/2006 (area covered 664.6 and 397.8 km^2 respectively), while on 03/03/2003 and on 25/03/2005 the floods were smaller (191.4 and 142.5 km^2 respectively) (Fig. 6). It must be noted that the inundated areas produced from the satellite images do not necessarily coincide with the maximum extent of each flood event, especially in case of the flood event during the period 09-25/03/2006.

The comparison between the flood hazard map produced and the inundated areas indicate the satisfactory performance of the model. More specifically, for each flood event the majority of the inundated area was characterized as areas of high or very high flood hazard (03/03/2003: 98.8%, 5/03/2005: 92.7%, 13/04/2006: 98.9%, 19/02/2010: 98.5%; Table 7), while in the not inundated areas of the riparian zone,

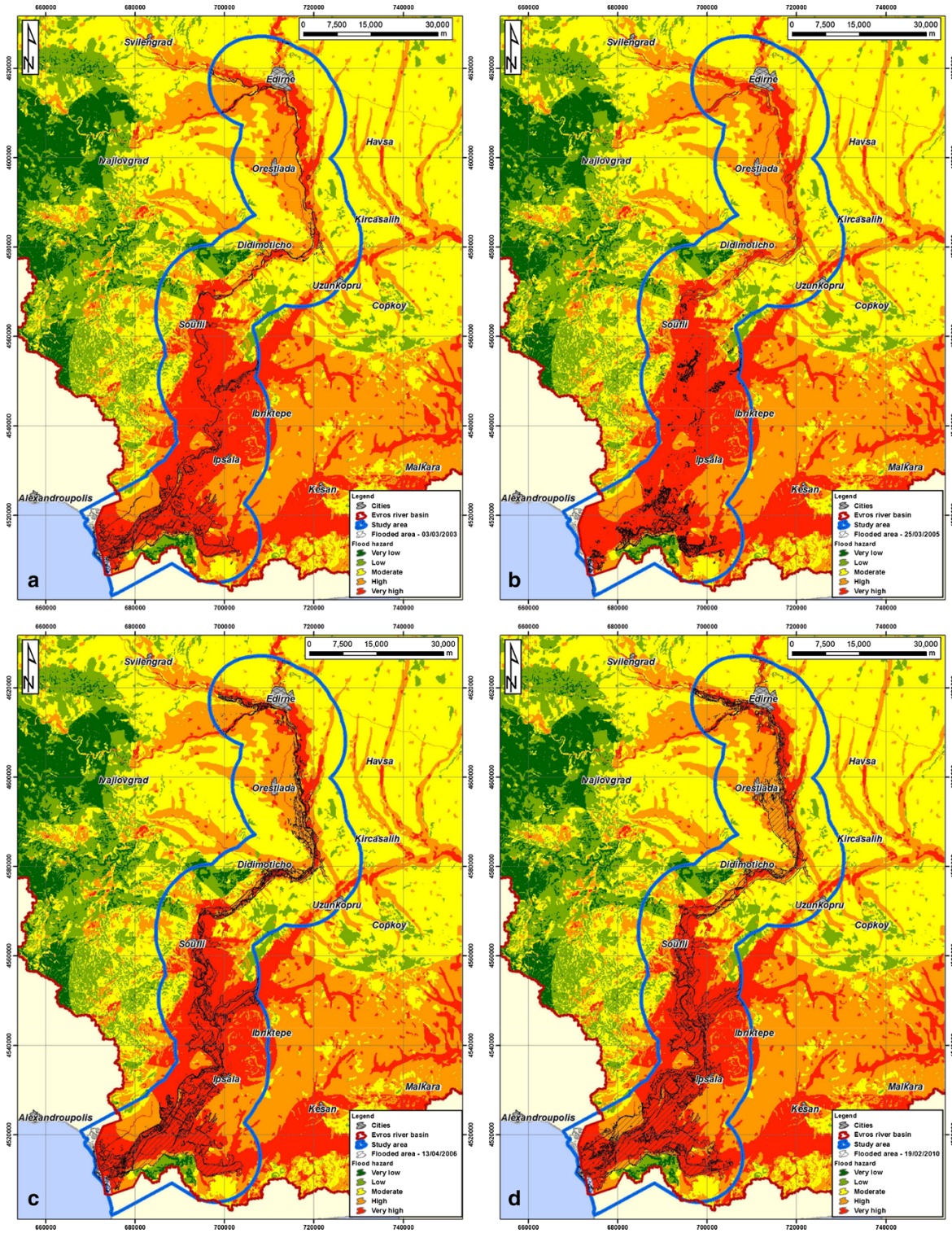

Figure 6
Evros river inundation map for the flood events on **a** 03/03/2003, **b** 25/03/2005, **c** 13/04/2006, **d** 19/02/2010

Table 7

Flood hazard classes and land uses of inundated and not inundated areas of each flood event examined

Flood event	03/03/2003		25/03/2005		13/04/2006		19/02/2010	
	Inundated (%)	Not inundated (%)	Inundated (%)	Not inundated (%)	Inundated (%)	Not inundated (%)	Inundated (%)	Not inundated (%)
Flood hazard classes								
Very low	0.00	1.50	0.10	1.50	0.00	1.60	0.00	1.80
Low	0.20	6.00	0.40	5.90	0.10	6.40	0.10	7.10
Moderate	1.00	29.90	6.80	29.10	1.00	31.90	1.40	35.10
High	9.80	29.40	21.00	28.50	16.00	29.90	22.60	29.60
Very high	89.00	33.30	71.80	35.00	82.90	30.10	75.90	26.50
Land uses								
Agricultural	57.80	80.50	72.30	79.50	76.60	79.50	79.80	79.00
Artificial surfaces	0.00	3.20	0.60	3.10	0.10	3.40	0.30	3.80
Forest and natural vegetation	1.60	13.00	4.50	12.70	1.00	13.90	1.70	15.00
Wetlands	40.50	3.40	22.60	4.70	22.30	3.20	18.30	2.20

Table 8

Flood hazard classes for each land use of the inundated areas of each flood event examined

Flood event	Land use	Flood hazard classes				
		Very low (%)	Low (%)	Moderate (%)	High (%)	Very high (%)
03/03/2003	Agricultural	0.0	0.0	0.7	8.5	90.8
	Artificial surfaces	0.0	0.0	0.0	0.0	100.0
	Forest and natural vegetation	0.0	9.9	16.8	22.1	51.1
	Wetlands	0.0	0.0	0.0	9.4	90.6
25/03/2005	Agricultural	0.0	0.1	7.1	21.8	71.0
	Artificial surfaces	0.0	0.0	2.4	41.5	56.1
	Forest and natural vegetation	1.7	8.7	36.0	12.2	41.3
	Wetlands	0.0	0.0	0.0	19.9	80.1
13/04/2006	Agricultural	0.0	0.0	0.8	17.2	82.0
	Artificial surfaces	0.0	0.0	0.0	0.0	100.0
	Forest and natural vegetation	0.0	5.0	26.5	13.3	55.2
	Wetlands	0.0	0.0	0.1	11.2	88.8
19/02/2010	Agricultural	0.0	0.1	1.1	26.2	72.6
	Artificial surfaces	0.0	0.0	0.0	12.9	87.1
	Forest and natural vegetation	0.4	3.2	28.0	20.8	47.6
	Wetlands	0.0	0.0	0.2	6.6	93.1

the flood hazard potential is lower (area characterized of high or very high flood hazard: 03/03/2003: 62.7%, 5/03/2005: 63.5%, 13/04/2006: 60.0%, 19/02/2010: 56.1%; Table 7). The inundated areas were mainly occupied by agricultural activities and wetlands and the not inundated areas by agricultural activities and at much smaller extent forest and natural vegetation (Table 7). For all flood events examined, the agricultural lands, artificial surfaces and wetlands inundated were characterized as areas of very high or high flood hazard (Table 8).

5. Conclusion

During the last decade the flood frequency especially downstream of Evros river has increased dramatically (Angelidis et al. 2010). The climatic and geomorphological conditions of Evros river basin combined with land use changes and poor management practices concerning mainly dams operation and irregular release of river flow, have increased flood risk (Papathanasiou et al. 2013). Especially Evros delta is an extremely vulnerable area

concerning flood hazard potential. In order to meet the European Directive 2007/60/EC requirements for the development of flood risk management plans, a GIS based, multi-criteria methodology for flood hazard mapping (Kourgialas and Karatzas 2011) was applied by adapting the method's hazard classes to the examined catchment's environmental conditions while maintaining the hazard weights and weighing rates of the original methodology. The latter have been estimated by a combination of expert judgement and a relevant weighting estimation method (Shaban et al. 2001). The satisfactory performance of this tool was verified, although some adjustments may improve further the model in Evros river basin specifically. The most vulnerable land uses against flood are agricultural lands, artificial surfaces and wetland.

GIS based multi-criteria decision analysis is lately widely used in complex decision problems (Papaioannou et al. 2015) and is quite popular because of its capacity to integrate a large amount of heterogeneous data and the ease in obtaining the weights of a large number of criteria (Chen et al. 2010). Nevertheless, some uncertainties arise due to subjective estimates, such as criteria selection and their thresholds and criteria weights (Chen et al. 2010; Raaijmakers et al. 2008). Based on the GWR results, the primary factors affecting mostly the flood hazard in Evros catchment is topography and land uses, followed by rainfall intensity, geology and flow accumulation. This is not completely in agreement with the weight of factors proposed by Kourgialas and Karatzas (2011), who considered the factor rainfall intensity less important than geology in flood producing. This methodology weakness could be attributed to the different flood producing mechanisms at Evros river basin comparing to the ones in the catchment the methodology was initially developed. More specifically, Evros river basin can be characterized as large-sized limiting the occurrence of flash flood events (Fotopoulos et al. 2010), while the hydrographic network is extensive.

Another important uncertainty issue arises on the choice of the optimal clustering technique, despite the fact that a respective number of GIS based multi-criteria decision analysis applications are using the Jenk's Natural Breaks method for classification of numeric-valued factors (e.g. Mallick et al. 2015; Pasqualini et al. 2011; Stefanidis and Stathis 2013). In order to produce hazard classes that contain data value groups with relatively large differences and to maximize "classing accuracy" (Smith 1986), the use of multiple clustering techniques is often necessary in preliminary analysis of flood hazard mapping (Papaioannou et al. 2015).

GIS based multi-criteria decision analysis lack the ability to comprise the temporal dimension of spatial distributed information and examine phenomena that change over time (Ratsiatou and Stefanakis 2001) comparing to other approaches, such as hydrological and hydraulic modelling. Nevertheless, GIS-based multi-criteria decision analysis can be applied in initial low-cost detection surveys of flood-prone areas (Papaioannou et al. 2015), to support decision-making and help stakeholders develop flood management plans.

The particular approach for estimating the flood-hazard areas of Evros river basin, combines the climatic, geomorphological and land use properties of the catchment to illustrate areas that are more prone to flooding in relation to others. It is a physically based approach and measures the protective function of each part of the basin based on its natural and anthropogenic characteristics. It has certain advantages and disadvantages compared to hydrologic modelling techniques as mentioned above. However, it is very useful in areas where hydrological data are completely absent, inefficient or have low credibility as well as where the hydrological systems are too complex to describe efficiently in a model (large catchments with many different water uses and stakeholders). This is particularly the case in transboundary catchments where all of the aforementioned problems are usually significantly enhanced and the cooperation between the catchment sharing countries is not always ideal.

6. *Discussion*

The flood risk management of transboundary water courses raises many challenges due to different approaches in strategic decision making, capacity and resources and due to the lack of a legal framework for

cooperation and the public participation and awareness (UNECE 2009). The European Directive 2007/60/EC, in line with Directive 2000/60/EC and international principles of flood risk management as developed notably under the United Nations Convention on the protection and use of transboundary water courses and international lakes, aims at effective flood prevention and mitigation practices. Especially at Evros river basin, where the countries involved are not all member states of the European Union, the challenges are even more complex. Only bilateral efforts have been made in the past and agreements have been signed related to water environmental cooperation including conservation of protected areas and management issues concerning flood protection at Evros transboundary river basin (Table 9). Important efforts have also be made in scientific level concerning flood risk management

Table 9

Existing agreements related to the management of Evros transboundary river basin

Country	Date	Basins concerned	Comments	References
GR, TR	1934	Maritsa/Evros/Meriç River	Agreement concerning the Control of Hydraulic Works on Both Banks of the Evros/Meriç River	1
GR, TR	1955	Maritsa/Evros/Meriç River	Agreement related to the construction of flood control measures	1
GR, TR	1963	Maritsa/Evros/Meriç River	Protocol on the Rehabilitation of the Meriç River Basin Forming the Significant Part of Turkish-Greek Border in Thrace	1
BG, GR	1964	Maritsa/Evros/Meriç River	Agreement on Cooperation between the People's Republic of Bulgaria and the Kingdom of Greece concerning the utilization of the waters of the rivers crossing the two countries	2
BG, TR	1968	Maritsa/Evros/Meriç, Arda/Ardas and Tundzha/Tundja/Tunca Rivers	The Agreement between the Republic of Turkey and the People's Republic of Bulgaria concerning Cooperation in the Use of the Waters of Rivers Flowing through the Territory of Both Countries established a Joint Commission authorized to settle any disputes which might have arisen	1
BG, GR	1971	Arda/Ardas, Maritsa/Evros/Meriç Rivers	FRESHWATERS AGREEMENTS Title and related joint body Agreement for the Establishment of the Greek-Bulgarian Committee for Cooperation in the Fields of Electric Energy and the Utilization of the Waters of the Rivers Crossing the Two Countries that was assigned to follow up the application of the 1964 agreement	1
GR, TR	1971	Maritsa/Evros/Meriç River	Prevention and means of peaceful settlement of disoute incintents in the cross border land and sea areas of River Evros/Meric	3
BG, TR	1975	Maritsa/Evros/Meriç, Arda/Ardas and Tundzha/Tundja/Tunca Rivers	Agreement between the Government of the Republic of Turkey and the Government of the People's Republic of Bulgaria on Long Term Economic, Technical, Industrial and Scientific Cooperation	1
BG, TR	1993	Tundzha/Tundja/Tunca River	Agreement on Assistance and Cooperation in the Field of Water for Reducing the Negative Effects of the Drought of 1993	1
BG, TR	1998	Maritsa/Evros/Meriç River	Agreement on Cooperation in the Fields of Energy and Infrastructure Between the Government of the Republic of Turkey and the Government of the Republic of Bulgaria	1
GR, TR	2001	Maritsa/Evros/Meriç and Arda/Ardas Rivers	Memorandum of Understanding Concerning Cooperation on Environmental Protection	1
BG, TR	2002	Maritsa/Evros/Meriç River	Protocol signed between the General Directorate of State Hydraulic Works of Turkey and the National Institute of Meteorology and Hydrology of Bulgaria for the installation, operation and maintenance of a flow observation telemetry station on the Maritsa River in Svilengrad, Bulgaria	1
BG, TR	2002	Maritsa/Evros/Meriç River	Agreement between the Ministry for the Environment, Physical Planning and Public Works of the Hellenic Republic and the Ministry of Environment and Water of the Republic of Bulgaria on cooperation in the field of environmental protection	2
GR, TR	2006	Maritsa/Evros/Meriç River	CBC for the prevention and control of floods in the riparian region of Evros/Meric	3

UNECE (2009), Mousmouti (2003), Skias and Kallioras (2007)

projects (e.g. INTERREG III A—PHARE CBC program between Bulgaria and Greece that focused on early warning in case of floods and accidental pollution and EC PHARE Cross-Border Cooperation between Turkey and Bulgaria which involved the creation of a hydrometeorological database and the installation of flood warning and water information systems), although none includes all three countries involved. In addition, no agreement exists that would provide a minimum inflow of freshwater into the delta, satisfying the water needs of the ecosystem as well as preventing salt water intrusion and siltation (Kramer and Schellig 2011).

On the other hand, many incidents underline the fact that most agreements, declarations or protocols between the riparian countries have not been fully implemented. Especially during the severe flood events in 2005, recriminations between Turkey, Greece and Bulgaria indicated the lack of a coordinated water management framework and a common flood prevention strategy. Although experts from the three countries agree that the primary cause of major flood events are specific flow patterns and extreme meteorological conditions (Kramer and Schellig 2011), the main argument raised on whether the poor water practices mainly of large Bulgarian reservoirs or whether the inappropriate floodplain management in Greece and Turkey intensify the phenomena and increase flood risk and vulnerability downstream.

The EU legislative framework provides the necessary means for efficient cooperation between the EU member states Greece and Bulgaria. The challenge rises in the cooperation between all the three countries involved. Accession Partnership between the EU and Turkey further provides opportunities for cooperation between Turkey and its European neighbors (Skias and Kallioras 2007). The first step for integrated water management of Evros river basin is the exchange of scientific knowledge and hydrological and water use data in order to develop a common database and the establishment of a common rather than a national flood forecasting and early warning system. These initiatives prerequisite also a common infrastructure establishment and an integrated water management plan for the entire river basin that will also focus on the environmental protection and conservation of natural resources. The political support for this effort and common legislation are preconditions.

References

Angelidis, P., Kotsikas, M., & Kotsovinos, N. (2010). Management of upstream dams and flood protection of the Transboundary River Evros/Maritza. *Water Resources Management, 24*, 2467–2484.

Arnoldus, H.M.J. (1980). An approximation of the rainfall factor in the Universal Soil Loss Equation. In M. De Boodt, and Gabriels, D. (Eds.), Assessment of erosion (pp. 127–132). Chichester: Wiley.

Becker, B. L., Lusch, D. P., & Qi, J. (2007). A classification-based assessment of the optimal spectral and spatial resolutions for Great Lakes coastal wetland imagery. *Remote Sensing of Environment, 108*, 111–120.

Bradshaw, C. J. A., Sodhi, N. S., Peh, K. S. H., & Brook, B. W. (2007). Global evidence that deforestation amplifies flood risk and severity in the developing world. *Global Change Biology, 13*, 2379–2395.

Brunsdon, C., Fotheringham, S., & Charlton, M. (1996). Geographically weighted regression: a method for exploring spatial non-stationarity. *Geographical Analysis, 28*, 281–298.

Castillejo-González, I. L., López-Granados, F., García-Ferrer, A., Peña-Barragán, J. M., Jurado-Expósito, M., de la Orden, M. S., et al. (2009). Object- and pixel-based analysis for mapping crops and their agro-environmental associated measures using QuickBird imagery. *Computers and Electronics in Agriculture, 68*, 207–215.

Charlton, M. and Fotheringham, S. (2009). Geographically weighted regression white paper (National Centre for Geocomputation National University of Ireland Maynooth, Maynooth, Co Kildare, Ireland) (http://www.geos.ed.ac.uk/∼gisteac/fspat/gwr/arcgis_gwr/GWR_WhitePaper.pdf).

Chen, Y., Yu, J., & Khan, S. (2010). Spatial sensitivity analysis of multi-criteria weights in GIS-based land suitability evaluation. *Environmental Modelling and Software, 25*, 1582–1591.

Darmouth Flood Observatory. (2014). Global Active Archive of Large Flood Events (http://www.dartmouth.edu/∼floods/Archives/index.html).

Davies, S.L. (2002). Discrepancy-based model selection criteria using cross-validation. Doctoral dissertation (University of Missouri-Columbia Department of Statistics, Columbia).

Davies, S. L., Neath, A. A., & Cavanaugh, J. E. (2005a). Cross validation model selection criteria for linear regression based on the Kullback-Leibler discrepancy. *Statistical Methodology, 2*, 249–266.

Davies, S. L., Neath, A. A., & Cavanaugh, J. E. (2005b). *On the minimum variance unbiasedness property of AICc and MCp*. Iowa City: Technical report (The University of Iowa Department of Biostatistics.

De Smith, M., Goodchild, M., & Longley, P. (2007). *Geospatial analysis: A comprehensive guide to principles, techniques and software tools*. Winchelsea: Troubador Publishing Ltd.

Debba, P., van Ruitenbeek, F. J. A., van der Meer, F. D., Carranza, E. J. M., & Stein, A. (2005). Optimal field sampling for targeting

minerals using hyperspectral data. *Remote Sensing of Environment, 99*, 373–386.

Dimitriou, E., Mentzafou, A., Zogaris, S., Tzortziou, M., Gritzalis, K., Karaouzas, I., et al. (2011). Assessing the environmental status and identifying the dominant pressures of a trans-boundary river catchment, to facilitate efficient management and mitigation practices. *Environmental Earth Sciences, 66*, 1839–1852.

Dimitriou, E., Moussoulis, E., Mentzafou, A., Tzortziou, M., Zeri, C., Colombari, E. and Markogianni, V. (2010). Environmental status assessment for Evros river basin. Final Technical Report (in Greek), (Hellenic Centre for Marine Research, Athens).

Erwin, K. L. (2009). Wetlands and global climate change: the role of wetland restoration in a changing world. *Wetlands Ecology and Management, 17*, 71–84.

European Commission Council. (2000). European Commission Council Directive 2000/60/EC of the European Parliament and of the Council of 23 October 2000 establishing a framework for Community action in the field of water policy. *Official Journal of the European Communities, L327*, 1–72.

European Commission Council. (2007). Directive 2007/60/EC of the European Parliament and of the Council of 23 October 2007 on the assessment and management of flood risks. *Official Journal of the European Union*, *L288*, 27–34.

European Environmental Agency—E.E.A. (2012), Corine Land Cover 2006 (http://www.eea.europa.eu).

Feyen, L., Barredo, J. I. and Dankers, R., Implications of global warming and urban land use change on flooding in Europe. In Water and Urban Development Paradigms—Towards an Integration of Engineering, Design and Management Approaches (ed. Feyen, J., Shannon, K., and Neville, M.) (Taylor and Francis, London 2009), pp. 217–225.

Fotheringham, S. (1992). Exploratory Spatial Data Analysis and GIS. *Environment and Planning A*, *24*, 1675–1678.

Fotheringham, S., & Brunsdon, C. (1999). Local forms of spatial analysis. *Geographical Analysis, 31*, 340–358.

Fotheringham, S., Brunsdon, C., & Charlton, M. (2002). *Geographically weighted regression: The analysis of spatially varying relationships*. Chichester: John Wiley & Sons Ltd.

Fotheringham, S., Charlton, M., & Brunsdon, C. (1996). The geography of parameter space: an investigation of spatial non-stationarity. *International Journal of Geographical Information Systems, 10*, 605–627.

Fotheringham, S., Charlton, M., & Brunsdon, C. (1997). Two techniques for exploring non stationarity in geographical data. *Geographical Systems, 4*, 59–82.

Fotheringham, S., & Rogerson, P. A. (1993). GIS and spatial analytical problems. *International Journal of Geographical Information Science, 7*, 3–19.

Fotopoulos, F., Makropoulos, C., & Mimikou, M. A. (2010). Flood forecasting in transboundary catchments using the open modeling interface. *Environmental Modelling and Software, 25*, 1640–1649.

Fournier, F. (1960). *Climat et érosion: la relation entre l'érosion du sol par l'eau et les précipitations atmosphériques*. Paris: Presses Universitaires de France.

Gass, L., Norman, L.M., Villarreal, M.L., Tolle, C., Coe, M. and Jamwal, P. (2013), A Test of Methods to Measure Vegetation Change Adjacent to Gabions in Sonora, Mexico using Landsat imagery, Presented at the Santa Cruz River Researcher's Day, Tucson Arizona.

Gemitzi, A., Petalas, C., Tsihrintzis, V. A., & Pisinaras, V. (2006). Assessment of groundwater vulnerability to pollution: a combination of GIS, fuzzy logic and decision making techniques. *Environmental Geology, 49*, 653–673.

General Directorate of Mineral Research and Exploration. (1961). Geological Map of Turkey, sheet Istanbul, 1:500,000, Ankara, Turkey.

Institute of Geology and Mineral Exploration—Division of General Geology and Economic Geology (1983), Geological Map of Greece, 1:500,000. Athens, Greece.

IPCC, Climate Change 2013—The Physical Science Basis—Working Group I Contribution to the Fifth Assessment Report of the Intergovernmental Panel on Climate Change - Summary for Policymakers. (Cambridge University Press, United Kingdom and New York 2013).

Keiner, L. E., & Yan, X.-H. (1998). A neural network model for estimating sea surface chlorophyll and sediments from thematic mapper imagery. *Remote Sensing of Environment, 66*, 153–165.

Khandekar, M. L. (2013). *The global warming—extreme weather link: a review of the state of science*. London: The Global Warming Policy Foundation.

Khandekar, M. L., Murty, T. S., & Chittibabu, P. (2005). The global warming debate: a review of the state of science. *Pure and Applied Geophysics, 162*, 1557–1586.

Kourgialas, N. N., & Karatzas, G. P. (2011). Flood management and a GIS modelling method to assess flood-hazard areas—a case study. *Hydrological Sciences Journal, 56*, 212–225.

Kramer, A. and Schellig, A. (2011). Meric River Basin: Transboundary Water Cooperation at the Border between the EU and Turkey, In Turkey's Water Policy National: National Frameworks and International Cooperation (ed. Kramer, A., Kibaroglu, A., and Scheumann, W.) (Springer Berlin Heidelberg, New York) pp. 229–249.

Kundzewicz, Z. W., Lugeri, N., Dankers, R., Hirabayashi, Y., Döll, P., Pińskwar, I., et al. (2010). Assessing river flood risk and adaptation in Europe-review of projections for the future. *Mitigation and Adaptation Strategies for Global Change, 15*, 641–656.

Lathrop, R. G., Lillesand, T. M., & Yandell, B. S. (1991). Testing the utility of simple multi-date thematic mapper calibration algorithms for monitoring turbid inland waters. *International Journal of Remote Sensing*, *12*, 2045–2063.

Malczewski, J. (2006). GIS-based multicriteria decision analysis: a survey of the literature. *International Journal of Geographical Information Science, 20*, 703–726.

Mallick, J., Singh, C. K., Al-Wadi, H., Ahmed, M., Rahman, A., Shashtri, S., et al. (2015). Geospatial and geostatistical approach for ground water potential zone delineation. *Hydrological Processes, 29*, 395–418.

Meyer, V., Scheuer, S., & Haase, D. (2009). A multicriteria approach for flood risk mapping exemplified at the Mulde river, Germany. *Natural Hazards, 48*, 17–39.

Michigan Technological University (2011), Geographic Information Science information and support - How to generate random points in ArcGIS, http://gis.mtu.edu/?p=127 (accessed on 27/02/2015).

Ministry of Environment Energy and Climate Change-Special Secretariat for Water, Flood directive 2007/60/EC: Preliminary Flood Risk Assessment (in Greek) (Athens, 2012).

Ministry of Forest and Water Management (2011), Official statistics (in Turkish) (http://www.milliparklar.gov.tr/Anasayfa/istatistik.aspx?sflang=tr).

Ministry of Infrastructure Transport and Networks—General Secretariat of Public Works—Earthquake Recovery Service (2014), Delimited flooded areas—credit measures (in Greek) (http://www.yas.gr/ApoList.asp?cat_apo_id=106).

Morgan, R. P. C. (2005). *Soil erosion and conservation* (3rd ed.). Oxford: Blackwell Publishing.

Mousmouti, M. (2003). Hellenic-Bulgarian Bilateral Agreements for the Protection and Use of Transboundary Watercourses (http://www.nomosphysis.org.gr/attachments/10/contribution7.mousmouti.doc).

Oliver, J. E. (1980). Monthly precipitation distribution: a comparative index. *Professional Geography, 32*, 300–309.

Openshaw, S. (1993). Exploratory Space-Time-Attribute Pattern Analysers, In Spatial Analysis and CIS (ed. Fotheringham A.S. and Rogerson P.A.) (Taylor and Francis, London), pp. 147–63.

Papaioannou, G., Vasiliades, L., & Loukas, A. (2015). Multi-criteria analysis framework for potential flood prone areas mapping. *Water Resources Management, 29*, 399–418.

Papathanasiou, C., Serbis, D., & Mamassis, N. (2013). Flood mitigation at the downstream areas of a transboundary river. *Water Utility Journal, 3*, 33–42.

Pasqualini, V., Oberti, P., Vigetta, S., Riffard, O., Panaiotis, C., Cannac, M., et al. (2011). A GIS-based multicriteria evaluation for aiding risk management *Pinus pinaster* Ait. Forests: a case study in Corsican Island, Western Mediterranean Region. *Environmental Management, 48*, 38–56.

Raaijmakers, R., Krywkow, J., & van der Veen, A. (2008). Flood risk perceptions and spatial multi-criteria analysis: an exploratory research for hazard mitigation. *Natural Hazards, 46*, 307–322.

Ratsiatou, I. and E. Stefanakis, Spatio-temporal multicriteria decision making under uncertainty, In Proceedings of the First International Symposium on Robust Statistics and Fuzzy Techniques in Geodesy and GIS (ed. Carosio, A. and Kutterer H.) (Zurich, 2001) pp. 169–174.

Schäuble, H., Marinoni, O., & Hinderer, M. (2008). A GIS-based method to calculate flow accumulation by considering dams and their specific operation time. *Computers & Geosciences, 34*, 635–646.

Semmler, T., & Jacob, D. (2004). Modeling extreme precipitation events-a climate change simulation for Europe. *Global and Planetary Change*, *44*, 119–127.

Skias, S. and Kallioras, A., Cross Border Co-operation and the Problem of Flooding in the Evros Delta, In Many Rivers to cross: Cross-border Co-operation in River Management (ed. Verwijmeren, J. and Wiering, M.) (Eburon Academic Publishers, Delft, The Netherlands 2007) pp. 119–143.

Skoulikidis, N. T., Economou, A. N., Gritzalis, K. C. and Zogaris, S., Rivers of the Balkans, In Rivers of Europe (ed. Tockner, K., Uehlinger, U., and Robinson, C. T.) (Academic Press, London 2009) pp. 421–466.

Smith, R. M. (1986). Comparing traditional methods for selecting class Intervals on choropleth maps. *Professional Geographer*, *38*, 62–67.

Stefanidis, S., & Stathis, D. (2013). Assessment of flood hazard based on natural and anthropogenic factors using analytic hierarchy process (AHP). *Natural Hazards, 68*, 569–585.

Turner, A. B., Colby, J. D., Csontos, R. M., & Batten, M. (2013). Flood Modeling Using a Synthesis of Multi-Platform LiDAR Data. *Water, 5*, 1533–1560.

UNECE (United Nations Economic Commission for Europe), Second Assessment of transboundary rivers, lakes and groundwaters (United Nations Publications, Geneva 2011).

UNECE (United Nations Economic Commission for Europe), Transboundary flood risk management: experiences from the UNECE region (United Nations Publications, New York and Geneva 2009).

U.S. Geological Survey (2003), Generalized Geology of Europe including Turkey (https://www.sciencebase.gov/catalog/).

WHO (World Meteorological Organization), Guide to hydrological practices. Volume I: Hydrology - From measurement to hydrological information (World Meteorological Organization, Geneva 2008).

YCEO - Yale Center for Earth Observation, Yale Institute of Biospheric Studies (2010). Index of CEO Documentation (http://www.yale.edu/ceo/Documentation/).

Zerger, A. (2002). Examining GIS decision utility for natural hazard risk modelling. *Environmental Modelling and Software, 17*, 287–294.

(Received June 23, 2014, revised August 30, 2016, accepted November 15, 2016, Published online November 25, 2016)